6-2003

RacB Regulates Cytoskeletal Function in *Dictyostelium* spp.

Eunkyung Lee
University of Connecticut, Storrs

David J. Seastone
Louisiana State University Medical Center

Ed Harris
University of Nebraska - Lincoln, eharris5@unl.edu

James A. Cardelli
Louisiana State University Medical Center

David A. Knecht
University of Connecticut, Storrs, knecht@uconn.edu

EUKARYOTIC CELL, June 2003, p. 474–485 Vol. 2, No. 3
1535-9778/03/$08.00+0 DOI: 10.1128/EC.2.3.474–485.2003

RacB Regulates Cytoskeletal Function in *Dictyostelium* spp.

Eunkyung Lee,[1]† David J. Seastone,[2] Ed Harris,[2] James A. Cardelli,[2] and David A. Knecht[1]*

Department of Molecular and Cell Biology, University of Connecticut, Storrs, Connecticut 06269,[1] and Department of Microbiology and Immunology, Louisiana State University Medical Center, Shreveport, Louisiana 71130[2]

Received 4 November 2002/Accepted 1 March 2003

Thus far, 14 homologues of mammalian Rac proteins have been identified in *Dictyostelium*. It is unclear whether each of these genes has a unique function or to what extent they play redundant roles in actin cytoskeletal organization. To investigate the specific function of RacB, we have conditionally expressed wild-type (WT-RacB), dominant negative (N17-RacB), and constitutively activated (V12-RacB) versions of the protein. On induction, cells expressing V12-RacB stopped growing, detached from the surface, and formed numerous spherical surface protrusions while cells overexpressing WT-RacB became flattened on the surface. In contrast, cells overexpressing N17-RacB did not show any significant morphological abnormalities. The surface protrusions seen in V12-RacB cells appear to be actin-driven protrusions because they were enriched in F-actin and were inhibitable by cytochalasin A treatment. The protrusions in V12-RacB cells did not require myosin II activity, which distinguishes them from blebs formed by wild-type cells under stress. Finally, we examined the functional consequences of expression of wild-type and mutant RacB. Phagocytosis, endocytosis, and fluid phase efflux rates were reduced in all cell lines expressing RacB proteins but the greatest decrease was observed for cells expressing V12-RacB. From these results, we conclude that like other members of the Rho family, RacB induces polymerization of actin but the consequences of activation appear to be different from other *Dictyostelium* Rac proteins so far investigated, resulting in different morphological and functional changes in cells.

Rho family proteins belong to the family of Ras-related small G proteins and play a key role in regulating the assembly and organization of actin filaments in response to stimuli. In addition, these small G proteins are involved in many cellular activities such as cell adhesion, cytokinesis, cell cycle progression, cell migration, chemotaxis, phagocytosis, endocytosis, and secretion (reviewed in reference 10). Thus far, six classes of Rho family proteins have been identified in humans, including Rho (RhoA, RhoB, and RhoC), Rac (Rac1, Rac2, Rac3, and RhoG), Cdc42 (Cdc42Hs, G25K, TC10, and Hs Chp), Rnd (Rnd1/Rho6, Rnd2/Rho7, and RhoE/Rnd3), RhoD, and TTF (2). It has been suggested that Rac1, RhoA, and Cdc42 have unique functions in inducing specific actin-containing structures in a cell. Activated forms of these proteins induce lamellipods, stress fibers, and filopods, respectively, when microinjected into Swiss 3T3 cells (16, 22, 24, 25). Nevertheless, it is not clear whether the 16 members of Rho family proteins have unique or overlapping functions. The functions of new members of Rho family proteins have been investigated. For example, TC10 was found to be an inducer of filopods and a binding partner of c-Jun amino-terminal kinase (JNK) and p21-activated kinase (PAK) (14, 15). A homologue of Cdc42, Hs Chp, was also identified as a binding partner of PAK and activator of JNK pathway but induces lamellipod formation (1). New members of the Rho family, Rnd1 and Rnd3, seem to inhibit the formation of stress fibers and focal contacts, leading to cell detachment from the substratum (17). Some of the functional specificity of the Rho family may come from cell type-specific expression. For example, Rac2 is restricted in expression to hematopoietic cells and has been shown to play a role in neutrophil chemotaxis (27).

Dictyostelium is a useful model system to study actin dynamics and cell motility and is a professional chemotactic phagocyte comparable to macrophages or neutrophils. Restriction enzyme-mediated integration screening identified RacE, a member of the Rho family, as an important regulator of cytokinesis (12). Thirteen other Rho family genes have been identified in *Dictyostelium* (4, 26); however, their specific functions are not yet understood. In a previous report, we showed that RacC overexpression leads to the formation of an unusual actin-containing protrusion at the cell surface and a threefold increase in phagocytosis while macropinocytosis rates were significantly reduced (29). RacF1 was shown to localize at macropinocytic cups, phagocytic cups, and cell-cell adhesions (26); however, the function of this protein is less clear. Recently, the function of Rac1 proteins was investigated by several groups. Overexpression of the constitutively active form of Rac1 generated lamellopodia, inhibited macropinocytosis (8, 19), and resulted in defects in growth and cytokinesis. Overexpression of the dominant negative form of Rac1 protein induced only modest effects on cell morphology and, in one study, inhibited chemotactic movement of cells (5). Together, these data indicate that Dictyostelium Rac1 proteins play a role in regulation of actin cytoskeleton and actin related activities comparable to that observed for mammalian cells.

* Corresponding author. Mailing address: Department of Molecular and Cell Biology, University of Connecticut, Storrs, CT 06269. Phone: (860) 486-2200. Fax: (860) 486-4331. E-mail: knecht@uconn.edu.

† Present address: Department of Cell Biology, Yale University School of Medicine, Boyer Center for Molecular Medicine, New Haven, CT 06510.

In this study we have generated cell lines that conditionally express wild-type and mutant forms of RacB to identify the role of RacB in actin cytoskeletal function and determine whether it shares functional redundancy with other *Dictyostelium* Rac proteins. *Dictyostelium* RacB has 50, 70, and 60% amino acid homology to *Dictyostelium* RacC, human Rac1, and human Cdc42, respectively. Our results suggest that RacB regulates polymerization of F-actin but in a manner that is different from the mechanism used by other Rac genes so far investigated. The spherical protrusions induced by the constitutively active form of RacB (V12-RacB) are dependent on actin polymerization but not on myosin II and are different from the petalopods produced by RacC overexpression. Expression of V12-RacB arrested cell growth, suggesting that RacB might also affect the cell cycle and/or cytokinesis. In addition, expression of V12-RacB dramatically reduced endocytosis, phagocytosis, and endosomal efflux while expression of WT-RacB and N17-RacB had lesser effects. We propose that RacB is normally involved in the control of cortical actin polymerization. The unique morphology of the V12-RacB-induced structures indicates that the pathway acting downstream of RacB is used to generate a unique form of cell protrusions distinguishable from those induced by RacC or Rac1 expression.

MATERIALS AND METHODS

Cell culture and transformation. Wild-type and mutant pVE2-HA-RacB were constructed by cloning full-length RacB cDNA into the *Sac*I site of pVE2ΔATG, thus placing RacB in-frame with a 10-amino-acid-encoding epitope tag from the hemagglutinin (HA) protein of influenza virus to make the vector, WT-RacB. This vector contained the discoidin I promoter, which can be induced with prestarvation factor (23) and repressed by growing cells in the presence of folate (3). Site-directed mutagenesis was performed to replace glycine 12 by valine in the RacB sequence to generate a constitutively active form of RacB named V12-RacB. Dominant negative RacB was generated by mutating Thr-17 to Asn and was named N17-RacB. These three constructs were transformed into Ax4 wild-type cells by electroporation (21). Transformants were selected with 20 μg of G418 (Sigma Chemical Co.) per ml in HL5 medium containing 1 mM folic acid (Research Organics) to repress RacB gene expression from the plasmid. G418-resistant cells were cloned on a lawn of *Klebsiella aerogenes,* and six colonies were picked to 24-well plates and maintained in folic acid and G418. Replicas of each clone were grown for 3 days in the presence of 20 μg of G418 per ml but in the absence of folic acid to induce expression of RacB. Levels of exogenously expressed RacB proteins were determined by Western blot analysis using an anti-HA antibody (Clonetech, Inc.) and rabbit anti-RacB antibody. Antibodies to RacB were generated by expressing RacB as a glutathione *S*-transferase fusion protein in *Escherichia coli.* Purified GST-RacB was injected into rabbits, and serum was collected. Three clones that expressed RacB proteins no more than twofold over endogenous levels were retained and maintained in the presence of 1 mM folic acid and 20 μg of G418 per ml at low density (less than 10^5 cells/ml). To induce protein expression from the discoidin promoter, cells were plated at low density on fresh HL5 medium lacking folic acid and G418 and grown for 24 to 36 h.

To visualize F-actin dynamics in cells expressing mutant RacB genes, pVE-HA-RacB, pVE-HA-N17RacB, and pVE-HA-V12RacB plasmids were transformed using G418 selection into Ax4 cells expressing the green fluorescent protein (GFP)-actin binding domain (ABD) fusion protein from a hygromycin-selectable plasmid (21). Resistant cells were cloned and maintained in the presence of 1 mM folic acid, 20 μg of G418 per ml and 25 μg of hygromycin (Calbiochem, Inc.) per ml at low density.

Cells lacking myosin II heavy chain (*mhcA*) were derived from HS1, in which the MhcA coding sequence was deleted (28). These cells were transformed with the pVE-HA-V12RacB vector and selected for G418 resistance under repressed conditions. The cells were then induced for V12-RacB expression as described above and in the figure legends.

Measurement of growth rate. Parental Ax4 and mutant cells were added to a 96-well plate in 100 μl of HL5 at 5×10^3 cells/ml. Every 10 to 14 h, cells were removed from a well and the cell density was measured using a hemocytometer. Two wells were used for each measurement, and the results were averaged.

Fluorescence microscopy. For phalloidin staining of F-actin, cells grown on a coverslip were fixed for 20 min with HL5 medium containing 1% formaldehyde, 0.1% glutaraldehyde (EM grade from Polysciences Inc.), 0.01% Triton X-100, and 1 μM TRITC-phalloidin (Sigma Co.). The fixation solution was made fresh at 2× concentration and mixed with an equal volume of cells in HL5. For nuclear staining, cells were fixed with 100% cold methanol for 15 min, washed with MCPB (10 mM Na_2HPO_4, 10 mM KH_2PO_4, 2 mM $MgCl_2$, 0.2 mM $CaCl_2$ [pH 6.5]), and then treated with 100 μg of RNase A per ml in TE (20 mM Tris, 1 mM EDTA [pH 7.5]). After a 1-h incubation, 10 μM propidium iodide was added and the mixture was incubated for an additional 30 min. The coverslip was washed with MCPB before being imaged.

Fluorescence images were collected using a Bio-Rad MRC-600 confocal laser-scanning microscope equipped with a 25-mW krypton-argon laser (Ion Laser Technology) attenuated with a 1% neutral-density filter. A 100× (1.30 NA) Neofluar oil immersion objective (Carl Zeiss Inc.) was used. Differential interference contrast (DIC) or phase contrast images and fluorescence images were collected simultaneously using the lowest direct scan rate and analyzed using NIH-Image (written by Wayne Rasband at the U.S. National Institutes of Health and available from the Internet by anonymous FTP from zippy.nimh.nih.gov.). Some images were further enhanced using Adobe Photoshop.

SEM. Scanning electron microscopy (SEM) was performed using the method of Fleurat-Lessard and Satter with minor modifications (8a). Cells were fixed for 30 min with HL5 containing 1% formaldehyde, 0.1% glutaraldehyde, and 0.01% Triton X-100. Further fixation was carried out using 2% glutaraldehyde in 50 mM HEPES buffer (pH 7.0) for 1 h and 1% O_sO_4 in 50 mM HEPES buffer (pH 7.0) for 4 h. After dehydration with ethanol, the cells were critical-point dried and coated with gold. A LEO982 (Carl Zeiss Inc.) field emission scanning electron microscope was used at an accelerating voltage of 2.0 kV.

Drug treatment. Butadione monoxime (BDM; Sigma) was made fresh in HL5 and used at 20 mM final concentration. Cells were grown on a coverslip for 2 days, and the drug was added for 30 min prior to imaging. Fields of cells were imaged using an inverted microsope (Carl Zeiss, Inc.) equipped with a 40× DIC objective and a charge-coupled device camera.

Induction of blebbing in wild-type and *mhcA* cells. Anoxia and electroporation were used in order to induce blebbing of cells. Cells were plated onto coverslips lying in the bottom of a petri dish. After overnight growth, a coverslip was removed and placed in a Rose chamber with the cells facing up. A circular Teflon spacer was placed on the top of the glass coverslip containing cells, HL5 medium was added, and then another coverslip was placed on the top of the Teflon spacer. The top part of the Rose chamber was placed on the top glass coverslip, and the assembly was screwed together to seal the chamber. Blebbing was reproducibly observed within 10 min after the chamber was sealed. In some experiments, cells were preincubated with 20 mM BDM for 10 min. The coverslip containing cells was then mounted in the Rose chamber as above with medium containing BDM.

Electroporation also induces blebbing of cells. The protocol used was the same as for transformation of cells with DNA (21). Briefly, cells were placed in a cold 0.1-cm cuvette in H-50 buffer (20 mM HEPES, 50 mM KCl, 10 mM NaCl, 1 mM Mg_2SO_4, 5 mM $NaHCO_3$, 1 mM Na_2HPO_4 [pH 7.0]) and pulsed at 0.85 kV and then 0.15 kV with a capacitance of 25 μF. The cells were removed from the cuvette and mixed with 500 μl of HL5 medium in an open Rose chamber immediately after electroporation, and imaging was started after 5 min.

Measurement of the number of pseudopods. Parental cells and V12-RacB cells were grown in a petri dish for 36 h to induce RacB expression and then detached from the substrate and shaken at 22°C for 10 min at 200 rpm. Cells were added to a petri dish, and images were captured in a focal plane above the dish surface, using 20× Hoffman modulation contrast microscopy, while the cells were settling to the bottom of the dish. The number of pseudopods on each cell was then determined.

Quantitation of F-actin. F-actin was quantified using a flow cytometer (Becton Dickson FACScaliber). Cells were grown in suspension culture starting at 2×10^5 cells/ml. After 24 to 36 h of growth, 1.5 ml of cells was collected and centifuged at $800 \times g$ for 5 min in the cold. The cells were resuspended in 200 μl of MCPB and fixed by addition of 2× fixation solution containing 0.5 μM of TRITC-phalloidin. The buffer was gently aspirated after overnight incubation at 4°C and exchanged for fresh MCPB without disturbing the cells at the bottom. Finally, the cells were resuspended in 1 ml of MCPB and analyzed in the cytometer.

Total and cytoskeletal actin were also quantified by staining of protein bands on sodium dodecyl sulfate SDS-polyacrylamide gels. The harvested cells were lysed with L buffer (20 mM PIPES [pH 7.5], 50 mM KCl, 5 mM EGTA, 0.2 mM

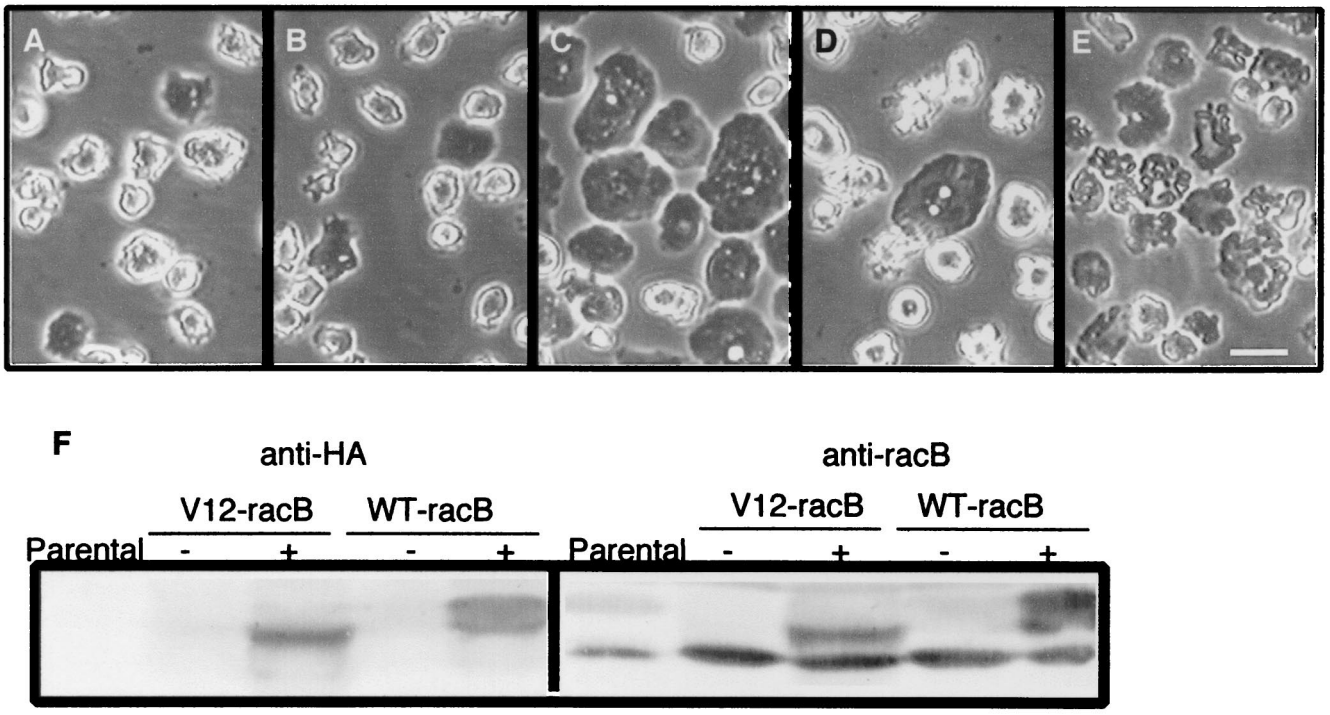

FIG. 1. Cell morphology changes induced by expression of RacB. (A to E) Cells were grown for 36 h in the presence or absence of folic acid, and phase-contrast images were captured. Wild-type Ax4 cells in the absence of folic acid (A), V12-RacB cells in fresh medium containing 1 mM folic acid (B), and WT-RacB cells (C), V12-RacB cells (D), and WT-RacC cells (E) in the absence of folic acid are shown. The morphology of WT-RacB, V12-RacB, and WT-RacC cells in the presence of folic acid is almost identical to that of parental cells but is dramatically changed on induction. WT-RacB cells became flattened, V12-RacB cells became detached with numerous protrusions on the cell surface, and WT-RacC cells became relatively flat with irregular contours on the surface. Bar, 20 μm. (F) Expression of WT-RacB and V12-RacB. Extracts of 2×10^5 parental, V12-RacB, and WT-RacB cells were harvested and run on an SDS–10% polyacrylamide gel. Expression of RacB was detected by rabbit polyclonal antibody against RacB (right panel) or by anti-HA antibody (left panel). In the presence of folate at low cell density (2×10^5 cells/ml), the recombinant protein was barely detectable (− lanes); however, it was induced twofold over the endogenous RacB level at high cell density in the absence of folic acid (+ lanes).

$MgCl_2$, 5 mM dithiothreitol, 1 mM ATP) containing 0.5% Triton X-100 and 5 μg each of the protease inhibitors leupeptin, chymostatin, and pepstatin per ml. After quantification of protein by the Bradford assay (Bio-Rad, Inc.), the lysates were centrifuged at 8,000 × *g* for 4 min and the cytoskeletal pellet was resuspended in L buffer and centrifuged again (7). Equal amounts of total-cell extract and threefold larger amounts of cytoskeletal fractions were loaded onto a 10% polyacrylamide gel. The protein bands were stained using Coomassie blue, and the actin band was quantified by densitometry using NIH-Image.

Endocytosis, exocytosis, and phagocytosis measurements. For phagocytosis, fluid-phase pinocytosis, and exocytosis assays, exponentially growing cells were harvested from T-175 tissue culture flasks (Sarstedt Inc.) and resuspended in growth medium at a titer of 3×10^6 cells/ml. For phagocytosis assays, cells were exposed to 1-μm-diameter fluorescent crimson latex beads (Molecular Probes) in HL5 medium at a concentration of 50 beads/cell. Cells and beads were shaken at 150 rpm in 25-ml Erlenmeyer flasks for 90 min. At various times, 1-ml aliquots of cells were harvested by centrifugation (1,000 × *g* for 5 min) and washed twice with cold HL5 growth medium and once with sucrose buffer (5 mM glycine, 100 mM sucrose [pH 8.5]). The cells were lysed with 0.5% Triton X-100, and the intracellular fluorescence was measured by spectrofluorimetry using a 625-nm wavelength for excitation and a 645-nm wavelength for emission. The fluorescence of each of the samples was normalized to total-cell protein to account for any differences in cell sizes between the strains. For fluid-phase pinocytosis assays, fluorescein isothiocyarate-dextran (70,000 M_r; Sigma) was incubated with shaking cultures of cells in growth medium to a final concentration of 2 mg/ml for 2 h. At various times, the cells were harvested and lysed with 0.5% Triton X-100 and the intracellular fluorescence was calculated with a spectrofluorimeter using 492 nm for excitation and 525 nm for emission. For exocytosis assays, cells were loaded for 3 h with 70,000 M_r FITC-dextran. The cells were washed twice with cold HL5 medium and resuspended in growth medium. At various times, they were harvested and lysed with 0.5% Triton X-100 and the intracellular fluorescence was determined as described above. To determine the percent fluorescence remaining in the cells, the fluorescence value at each time point was compared with the fluorescence at time zero, which was given a value of 100%.

RESULTS

Alterations in RacB function in *Dictyostelium* cells. To examine the function of RacB in *Dictyostelium,* cell lines were generated expressing wild-type protein (WT-RacB), a dominant negative version of the protein (DN-RacB), or a constitutively active version of RacB (V12-RacB) under the control of the inducible discoidin promoter. This promoter is repressed in the presence of folate at low cell density ($<5 \times 10^5$ cells/ml) and induced by high cell titer ($>10^6$ cells/ml) or by conditioned medium in the absence of folate (3). The proteins were tagged with HA at the N terminus to allow detection of exogenously expressed proteins. In addition, anti-RacB antibody was used to compare the expression level of the exogenous proteins relative to endogenous proteins. In the presence of folate at low cell density, all three tagged forms of the proteins were undetectable. However, after cells were grown to a high cell density (10^6 cells/ml) in the absence of folic acid, WT-RacB, N17-RacB, and V12-RacB were induced 200, 50, and 80% respectively, over the level of endogenous RacB (Fig. 1F and our unpublished results).

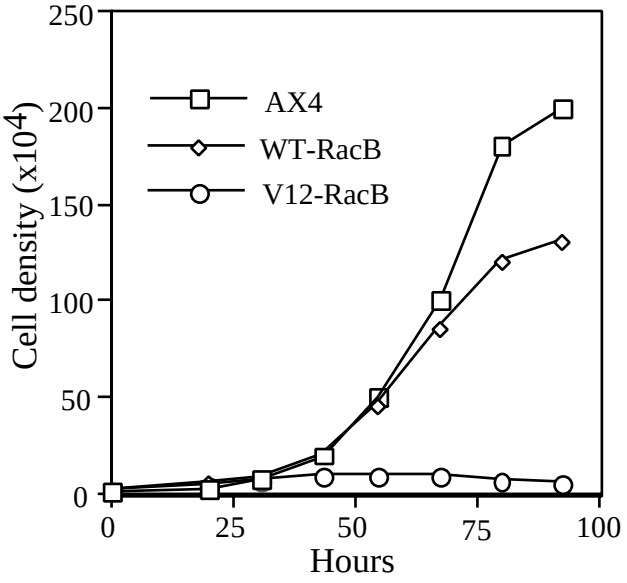

FIG. 2. Growth of parental, WT-RacB, and V12-RacB cells. Equal numbers of cells from each cell line were added to wells of a microtiter plate. Cells from two wells were taken every 10 to 14 h to determine the average cell density. Parental Ax4 cells have an 11-h generation time, while V12-RacB cells stopped growing 36 h after folic acid removal. WT-RacB cells had a slightly lower growth rate.

RacB expression alters cell morphology and growth. The morphology of WT-RacB, N17-RacB, and V12-RacB cells under conditions where exogenous proteins were not expressed was virtually identical to that of wild-type cells (Fig. 1A and B). On induction, WT-RacB and V12-RacB cells underwent a dramatic shape change whereas the N17-RacB cells appeared unchanged (our unpublished results). Cells expressing WT-RacB flattened out until they were almost in contact with each other (Fig. 1C). Although a proportion of cells expressing V12-RacB showed a flattened morphology like WT-RacB cells, the majority of cells became detached from the dish and formed numerous protrusions on the cell surface (Fig. 1D). The average number of protrusions on each cell was increased to about 9.8 ± 2.8 (n = 50), compared to 3.3 ± 1.1 on wild-type AX4 cells (n = 56). To compare the phenotype induced by V12-RacB expression with petalopods induced by WT-RacC expression (29), we also imaged a cell line expressing WT-RacC. Unlike cells expressing V12-RacB, WT-RacC cells remained attached to the dish and were relatively flat, with protrusions on the surface that are morphologically distinguishable from V12-RacB-induced protrusions (Fig. 1E).

To determine if cells expressing different forms of RacB proteins could grow and divide normally, wild-type AX4 and mutant cells were grown in a 96-well plate in the absence of folic acid and the titer was recorded over time. Surprisingly, cells expressing V12-RacB stopped dividing, so that the cell density did not increase for at least 36 h after folic acid removal (Fig. 2). Some cells lysed during the 3 days of growth under the induced conditions; however, the majority of the cells were viable since more than 80% of the cells could grow to form colonies on a bacterial lawn (our unpublished results). In contrast, the growth rate was not significantly inhibited in cells overexpressing WT-RacB (Fig. 2) or N17-RacB (our unpublished results). Since a more dramatic effect was observed in cells expressing V12-RacB, further studies were focused on functional characterization of V12-RacB cells.

To investigate whether the population of V12-RacB cells stopped growing or were inhibited in cytokinesis, nuclear stains of the mutant and wild-type cells were performed using propidium iodide after the cells had grown for 3 days under induced conditions (Fig. 3). The average number of nuclei in parental Ax4 cells was 1.7, and 87% of cells contained one or two nuclei per cell (n = 157). On the other hand, only 26% of

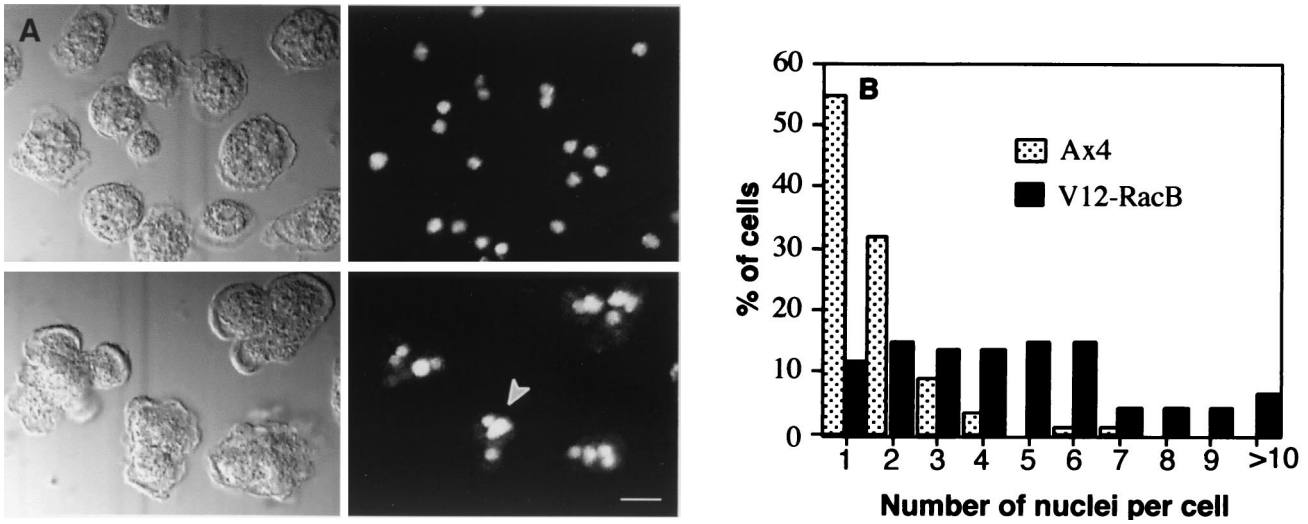

FIG. 3. Nuclear staining of parental and V12-RacB cells. (A) Cells were grown for 3 days under induced conditions and stained with 1 μM propidium iodide to visualize nuclei. Left panels are DIC images, and right panels show the nuclear staining. The upper panels are wild-type cells, and the lower panels V12-RacB cells. The arrowhead indicates heterogeneous sizes of nuclei in V12-RacB cells. (B) The number of nuclei was counted from 157 parental and 97 V12-RacB-expressing cells. In parental cells, 87% contain one or two nuclei, as opposed to 26% in V12-RacB population. The number of nuclei in cells expressing V12-RacB ranged from 1 to 15, compared to 1 to 5 in wild-type cells.

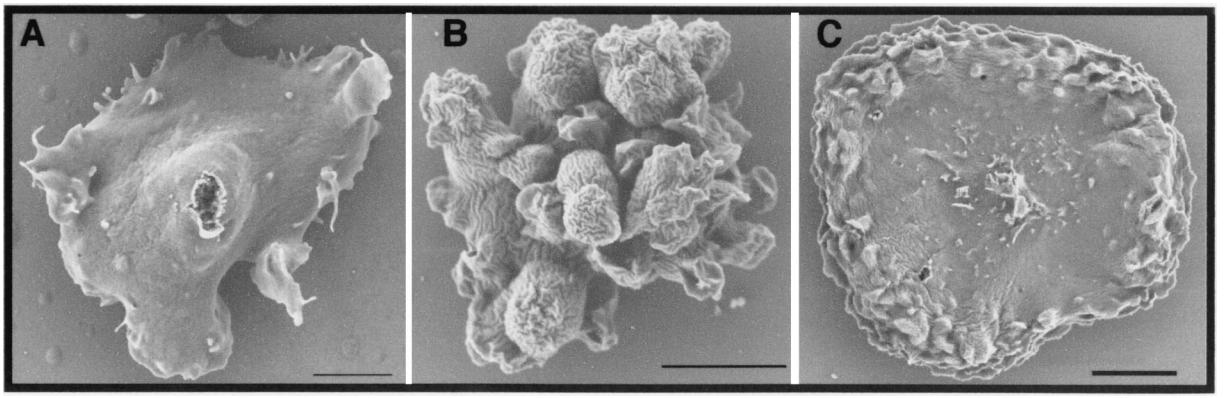

FIG. 4. Scanning electron micrographs of parental and V12-RacB cells. Cells were grown on glass coverslips and prepared for SEM after 2 days of growth in the absence of folic acid. (A) Parental cells have a thick center with protrusions at the cell edge. (B) V12-RacB cells have numerous irregular protrusions on the cell surface. (C) Some V12-RacB cells remain flattened on the surface and contain numerous protrusions at the cell edges. Bar, 5 μm.

V12-RacB cells had one or two nuclei, and the average number of nuclei was 4.7 ($n = 97$). It has been shown that cells lacking myosin II activity can continue nuclear division when cytokinesis is blocked, so that they become large and multinucleated with over 100 nuclei in a cell (6, 11). The fact that the V12-RacB cells stop increasing in number yet do not become enlarged or dramatically multinucleated implies that expression of V12-RacB blocks cell growth and/or the cell cycle rather than just cytokinesis. Interestingly, the sizes of nuclei in the V12-RacB cells were heterogeneous (Fig. 3A), with nuclei both larger and smaller than those in parental cells. These results might indicate that nuclear division was also affected by expression of V12-RacB.

To visualize the changes in the three-dimensional cell shape of the mutant cells, SEM was performed. In parental cells, the center of the cell is thick and the edges are relatively thin so that the whole cell has a conical shape (Fig. 4A). Consistent with the observations made by light microscopy, many cells expressing V12-RacB formed numerous cylindrical or spherical protrusions on the cell surface (Fig. 4B). Some of the V12-RacB cells remained flattened on the surface, and these cells also contained numerous protrusions, but only at the cell edges instead of over the entire cell surface (Fig. 4C).

Nature of the surface protrusions on V12-RacB cells. The spherical surface protrusions found on V12-RacB-expressing cells might be formed by a variety of mechanisms. They could be actin polymerization-dependent pseudopods, water-filled membrane blebs, or a deformation of the actin cortex and plasma membrane. Blebs are presumed to be formed by hydrostatic pressure at areas where the association of the cortex with the membrane is weakened and the membrane balloons out from the actin cortex. To investigate the spherical structures formed by V12-RacB cells, the dynamic process of blebbing in wild-type cells was observed under different conditions. Cells transiently form blebs when depleted of oxygen, such as when placed in a sealed chamber (Fig. 5A and E) or following electroporation (our unpublished results). The morphology of the spherical blebs in both cases appears very similar (similar size and shape, and devoid of vesicles).

It has been shown that myosin plays a role in apoptotic blebbing of mammalian cells (13). Since the anoxic blebs and the spherical protrusions formed by V12-RacB both resemble apoptotic blebs, we examined the role of myosin II in these processes. Cells lacking myosin II heavy chain (*mhcA*) were electroporated or placed in a sealed chamber. Unlike parental control cells (Fig. 5A and E), *mhcA* cells did not form blebs under either of these conditions (Fig. 5C and G and our unpublished results). The role of myosin in bleb formation was also confirmed by using BDM, an inhibitor of myosin ATPases (13). Pretreatment with BDM for 10 min blocked the formation of blebs in wild-type cells that were placed in sealed chamber (our unpublished results). To examine whether spherical protrusions formed by V12-RacB are also myosin II dependent, V12-RacB was introduced into *mhcA* cells. When expression of V12-RacB was induced, protrusions began to form that were similar to those found in wild-type cells expressing V12-RacB (Fig. 5H). Thus, unlike apoptotic membrane blebs and stress-induced blebs, spherical protrusions formed by V12-RacB cells do not require myosin II function. The most likely mechanism for formation of the V12-RacB protrusions is actin polymerization. Consistent with this hypothesis, cytochalasin A blocks the formation of these protrusions (Fig. 5B and F) but not the formation of blebs (our unpublished results).

Changes in the actin cytoskeleton. Since the V12-RacB cells have increased numbers of protrusions, it is possible that the amount of F-actin in these cells might be elevated. To test this hypothesis, cells were fixed and stained with TRITC-phalloidin and the level of fluorescence was examined using flow cytometry. From forward-scatter data, it was apparent that cell size was generally increased in V12-RacB cells (Fig. 6A). This is presumed to be due to a defect of cytokinesis and karyokinesis in V12-RacB cells (Fig. 2 and 3); however, it is possible that it reflects the altered shape of the cells. When cells of the same forward-scatter range (R3 or R5) were examined for their fluorescence intensity, V12-RacB cells showed a 77% (R3) and 56% (R5) increase in mean fluorescence (Fig. 6C and D; Table 1). This indicates that V12-RacB expression leads to an increase in the amount of F-actin in cells. In addition, the amount of F-actin associated with the Triton-insoluble cy-

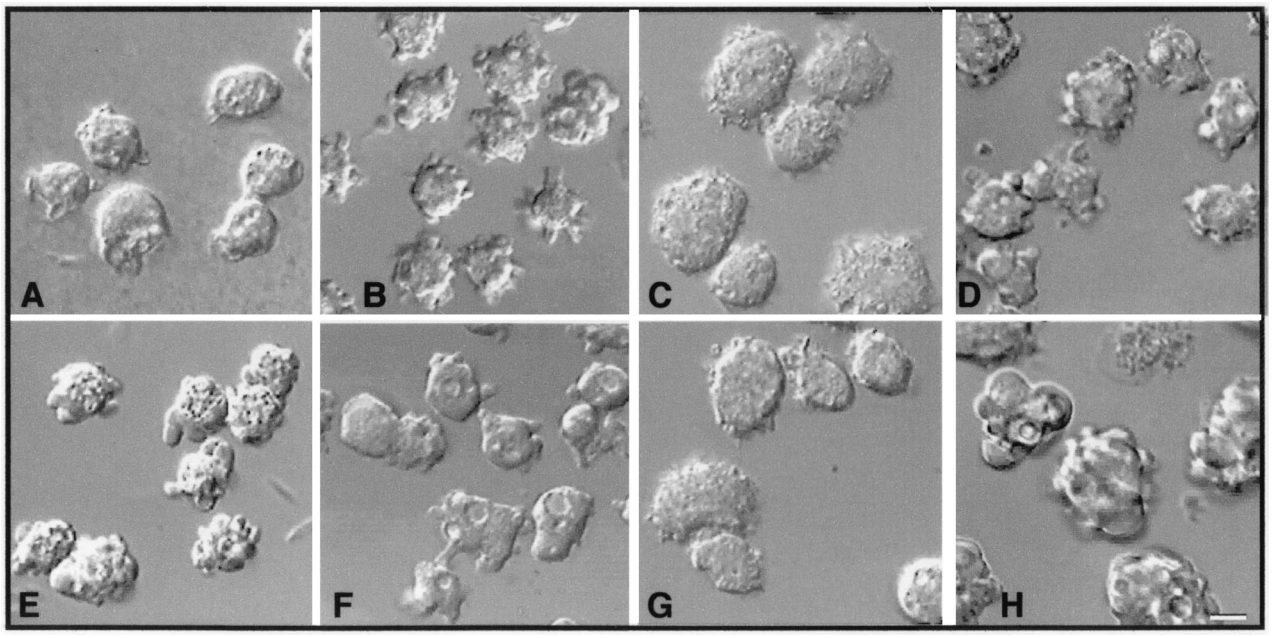

FIG. 5. Comparison of V12-RacB protrusions to stress-induced blebs. (A and E) Cells were sealed between two coverslips in a Rose chamber and imaged at 1-min intervals. The cells stopped moving after 5 to 10 min in the sealed chamber and began to form blebs. Control cells before sealing (A) and after 20 min in the chamber (E) are shown. (B and F) V12-RacB (Ax4 parental) cells contained surface protrusions (B), but after treatment with 10 μM cytochalasin A for 5 min, the protrusions were lost from the surface (F). (C and G) Myosin null cells (*mhcA*) before sealing (C) and after a 20-min (G) or 1-h incubation. The cells did not show any blebbing after incubation (our unpublished results). (D and H) Expression of V12-RacB was induced for 3 days in JH10, a parental cell line of *mhcA* cells (D), and in *mhcA* cells (H). Surface protrusions were induced in both cell lines. Bar, 5 μm.

toskeleton was increased twofold relative to parental cells (from 30% to nearly 59%) in V12-RacB cells (Fig. 6E; Table 1). The increase in the amount of F-actin was not accompanied by an increase in the amount of total actin, thus, the ratio of F- to G-actin was increased in V12-RacB cells. These results confirm that V12-RacB induces actin polymerization in these cells.

To examine the organization of the F-actin cytoskeleton, V12-RacB cells were fixed and stained with TRITC-phalloidin and confocal *z* sections were acquired. Parental cells showed a peripheral actin cortex, actin-enriched protrusions, and actin-rich crown structures on the dorsal surface (Fig. 7A). The surface protrusions of V12-RacB cells seen by light microscopy and SEM were also visible under fluorescence microscopy and were enriched in F-actin throughout their volume but especially at the tips of protrusions (Fig. 7B). In these cells, the circular actin cortex was clearly visible and the many small actin-rich protrusions appeared to extend from this underlying cortex. Cells expressing WT-RacC were also examined to determine whether the petalopods induced in WT-RacC cells differed from the V12-RacB-induced protrusions. WT-RacC cells also showed extensive F-actin staining at the periphery of the cell, but the morphology of the actin cortex was dramatically different (Fig. 7C). In these cells, there appeared to be no regular underlying circular actin cortex with protrusions added on; rather, the entire actin cortex appeared distorted into the irregular shapes of the petalopods. Thus, RacB-induced protrusions and RacC-induced petalopods appear to be different actin-containing structures.

TABLE 1. F-actin quantitation in cells

Cell line	Mean fluorescence intensity[a]	Total amt of F-actin[b]	% of total in cytoskeleton[c]	Fold increase
Ax4 parental-R3	488.63			
V12-RacB-R3	865.35			1.77
Ax4 parental-R5	692.88			
V12-RacB-R5	1,082.03			1.56
AX4 parental		1	30.1 ± 4	
V12-RacB		1.05 ± 0.12	58.9 ± 4	1.96
WT-RacB		0.98 ± 0.02	39.9 ± 8	1.33

[a] The mean intensity of fluorescence in two different size gates (R3 and R5) is shown for each cell line.

[b] Total F-actin (expressed relative to the amount in parental cells) was determined by staining fixed cells with fluorescent phalloidin and then quantifying bound dye by flow cytometry.

[c] Cytoskeletal actin was quantified by lysing cells, pelleting the cytoskeleton, and determining the amount of actin associated with the pellet by densitometry of Coomassie blue-stained SDS-polyacrylamide gels.

To visualize the changes in the actin cytoskeletal dynamics, WT-RacB and V12-RacB constructs were transformed into cells that constitutively express GFP-ABD. This fusion protein binds specifically to F-actin structures present in living cells and allows dynamic changes in F-actin localization to be visualized (20). In confocal time-lapse movies, wild-type cells expressing GFP-ABD showed staining of the cortex and pseudopods, as well as crown structures on the dorsal surface (Fig. 8A). The formation of pseudopods was accompanied by a local increase in the GFP-ABD signal (Fig. 8A). This increased

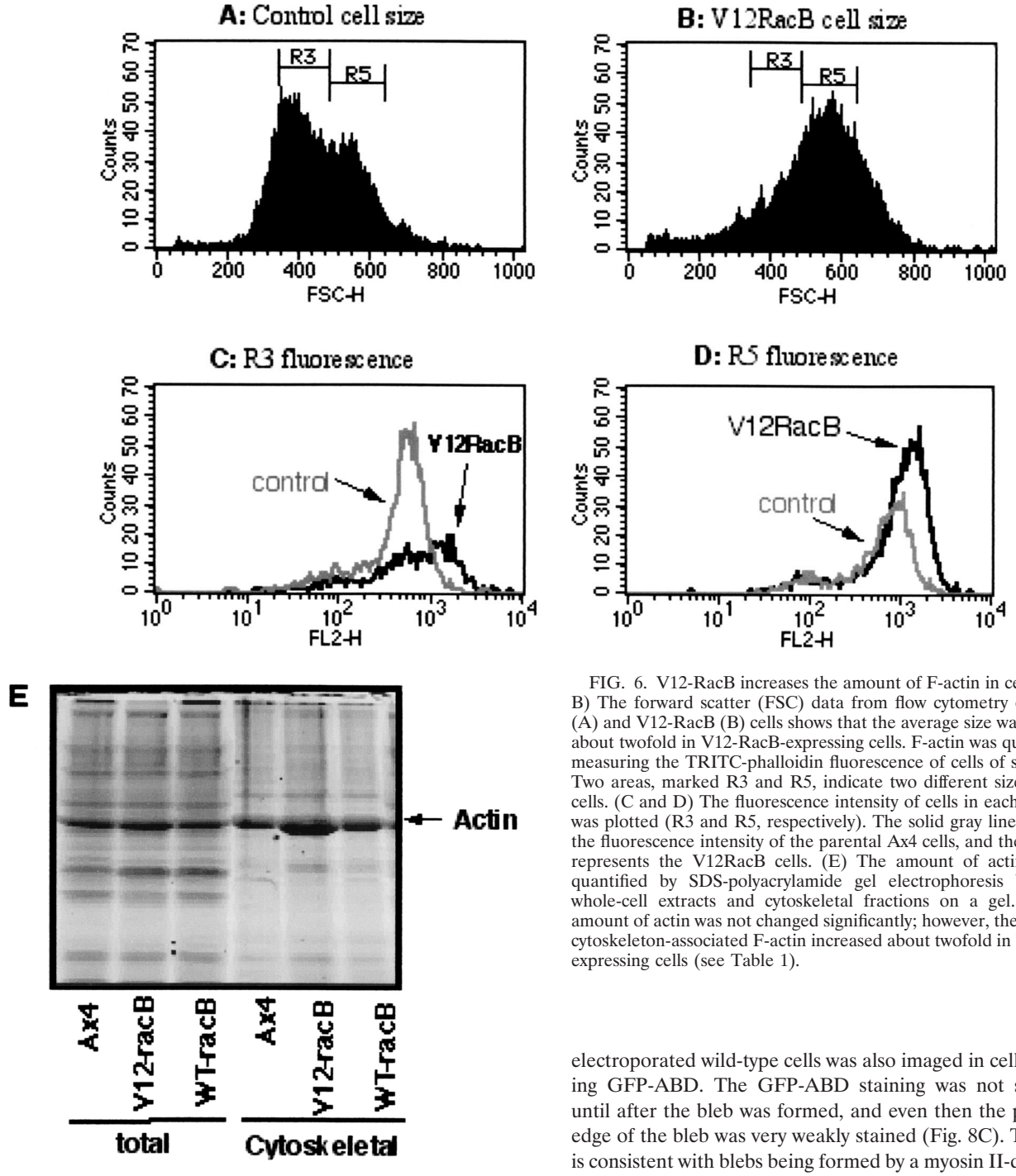

FIG. 6. V12-RacB increases the amount of F-actin in cells. (A and B) The forward scatter (FSC) data from flow cytometry of parental (A) and V12-RacB (B) cells shows that the average size was increased about twofold in V12-RacB-expressing cells. F-actin was quantified by measuring the TRITC-phalloidin fluorescence of cells of similar size. Two areas, marked R3 and R5, indicate two different size ranges of cells. (C and D) The fluorescence intensity of cells in each size range was plotted (R3 and R5, respectively). The solid gray line represents the fluorescence intensity of the parental Ax4 cells, and the black line represents the V12RacB cells. (E) The amount of actin was also quantified by SDS-polyacrylamide gel electrophoresis by loading whole-cell extracts and cytoskeletal fractions on a gel. The total amount of actin was not changed significantly; however, the amount of cytoskeleton-associated F-actin increased about twofold in V12-RacB-expressing cells (see Table 1).

fluorescence intensity due to association of the GFP probe occurs nearly as rapidly as the protrusion can be observed in the transmitted light image and initially fills the entire protrusion. In V12-RacB-expressing cells, many small spherical protrusions appeared and disappeared over time (Fig. 8B). GFP-ABD staining was found mostly at the edges of structures, and unlike wild-type cell protrusions, the intensity was roughly the same as that of the nearby cortex (Fig. 8B). Bleb formation of electroporated wild-type cells was also imaged in cells expressing GFP-ABD. The GFP-ABD staining was not significant until after the bleb was formed, and even then the peripheral edge of the bleb was very weakly stained (Fig. 8C). This result is consistent with blebs being formed by a myosin II-dependent mechanism while V12-RacB protrusions are formed by an actin polymerization-dependent mechanism. The petalopods produced by WT-RacC-expressing cells were also examined by GFP-ABD staining. The distorted cortex of WT-RacC cells was either pushed outward or pulled inward over time so that there was no clear distinction between the cortex and protrusions (Fig. 8D). Rather, the whole cortex and protrusions are contiguous so that the cell shape is contoured. Compared to this, V12-RacB cells showed relatively local outward protrusions, leading to an increase in the number of protrusions but of a size that is comparable to that of wild-type protrusions.

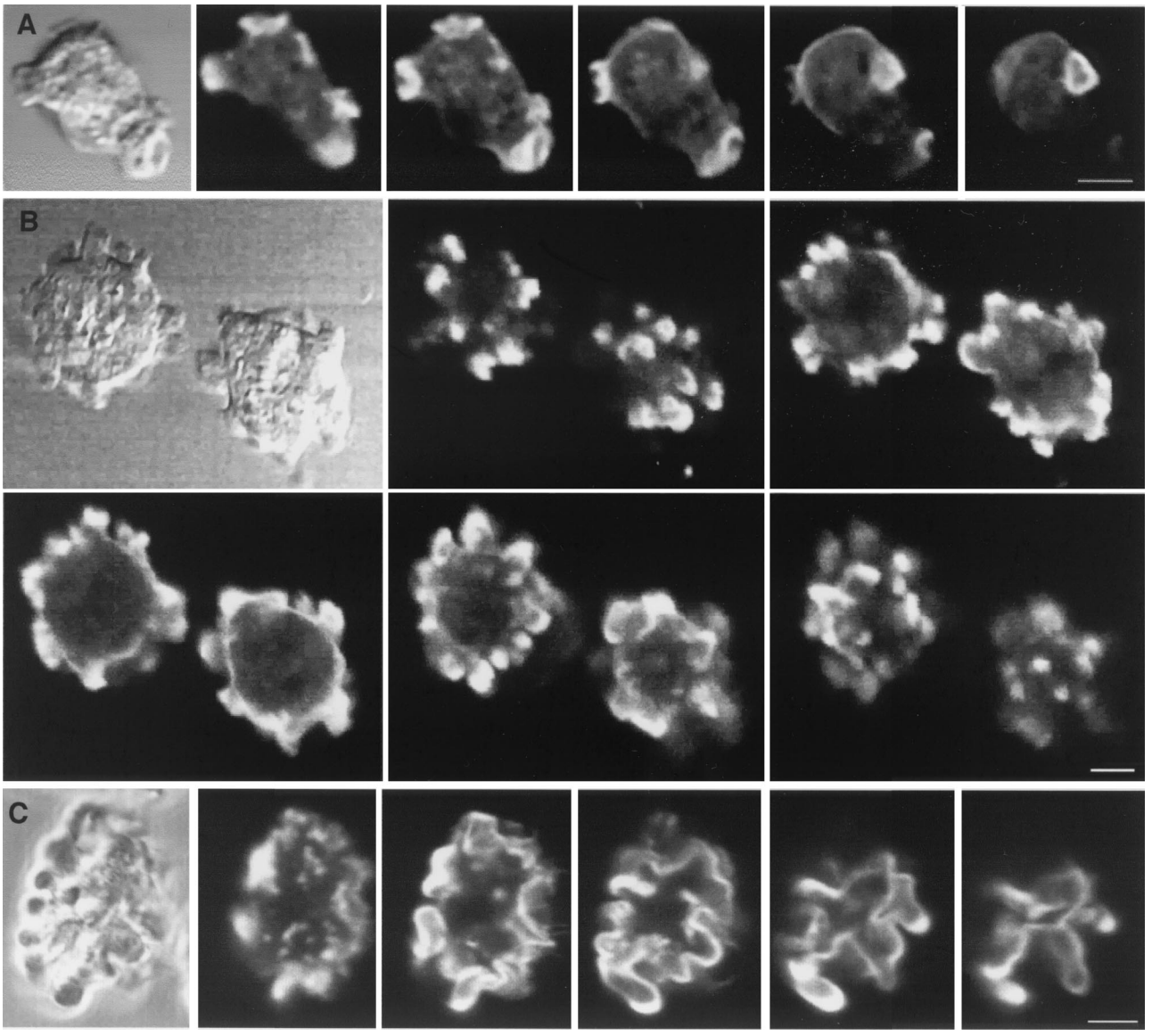

FIG. 7. Three-dimensional localization of F-actin. Cells were fixed and stained with TRITC-phalloidin, and confocal *z* sections were acquired. (A) Wild-type cells. Images are shown at 1.4-μm *z* intervals. (B) V12-RacB cells. Images are shown at 3-μm *z* intervals. Note that the protrusions on the cell surface are enriched in F-actin. (C) WT-RacC cells. Images are shown at 1.5-μm *z* intervals. Note that these deformations of the cortex are not actin filled. Bar, 5 μm.

Role of RacB in endolysosomal membrane trafficking. To determine if the mutant cell lines were altered in endocytic and exocytic processes, we measured rates of phagocytosis, endocytosis, and fluid-phase efflux. The rate of phagocytosis was dramatically reduced in the V12-RacB and N17-RacB cell lines compared to wild-type cells (Fig. 9A). In fact, the rate of internalization of particles into V12-RacB cells was only marginally greater than background levels. In contrast, internalization rates of particles into WT-RacB cells were only slightly reduced relative to the rates observed for control cells. WT-RacB and N17-RacB cells internalized fluid at 50% of the rate of control cells (Fig. 9B), while V12-RacB cells internalized fluid at only 25% of the rate of control cells. For all cell lines, internalization rates were linear for 60 min.

To measure fluid-phase efflux rates, cells were loaded with TRITC-dextran for 2.5 h, washed, and resuspended in fresh HL5 medium and the remaining fluorescence was determined over time. The rate of efflux of the fluid phase marker was dramatically lower in V12-RacB cells than in control cells. For instance, 50% of the fluorescent fluid phase was released from control cells after 40 min of chase whereas 110 min was required for release of 50% of the fluid from V12-RacB cells. In contrast, fluid-phase release was only slightly affected in WT-RacB cells; 55 min of chase was required for 50% release. The N17-RacB cells were only slightly less efficient than the WT-RacB cells in releasing fluid.

DISCUSSION

Rho family proteins are important regulators of F-actin polymerization. Thus far, 15 human and 16 *Dictyostelium* Rho

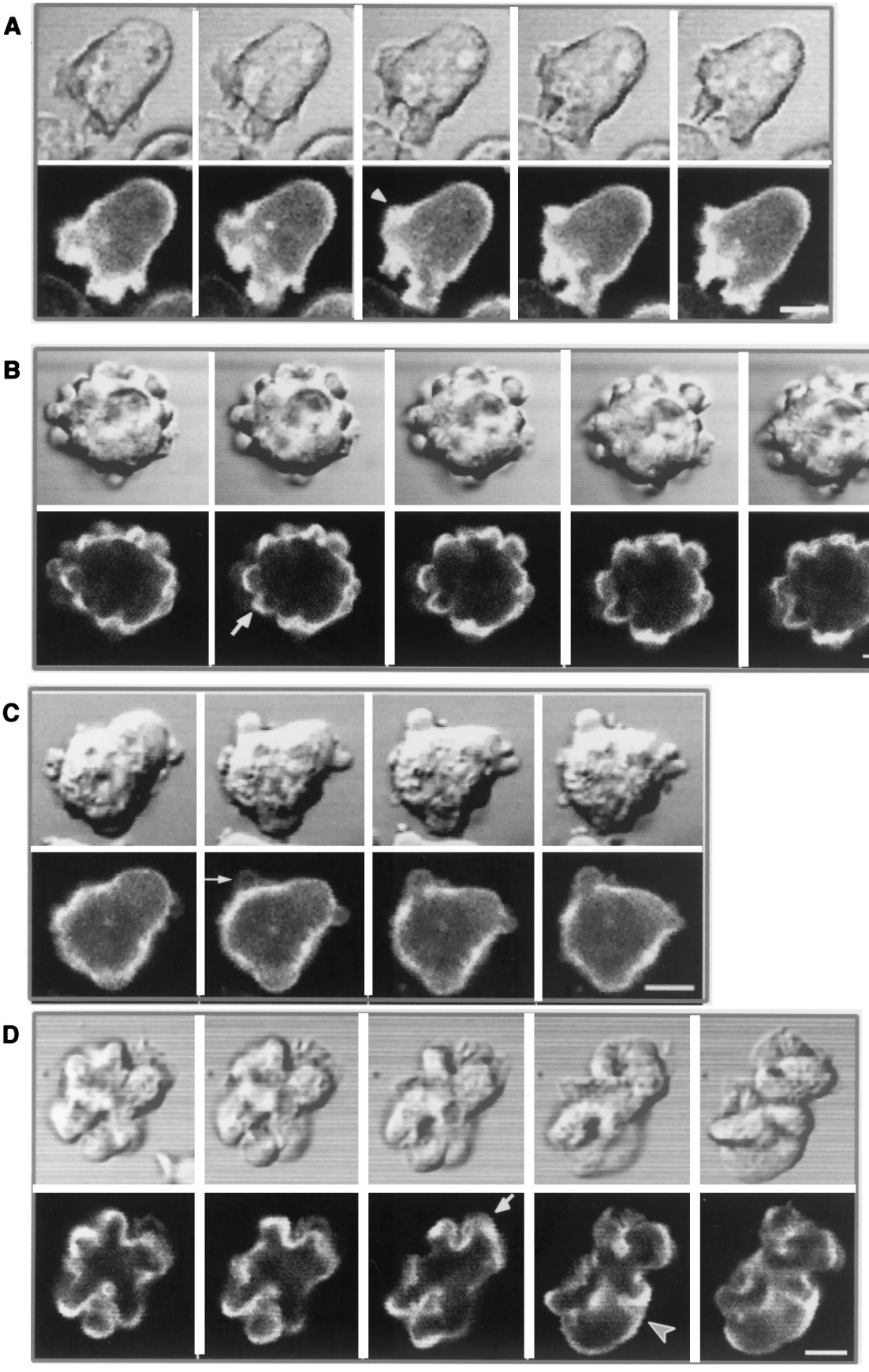
A
B
C
D

family proteins have been identified (4, 26) and have been found to have 50 to 90% amino acid sequence homology. Despite this sequence homology, it is not clear if each of the *Dictyostelium* Rho family GTPases plays a unique role in actin polymerization and other cellular processes, as proposed for human Rac1, RhoA, and Cdc42 in Swiss 3T3 cells, or if they function in a redundant capacity. RacE was reported to be an important regulator of cytokinesis (12) as well as to be essential for integrity of cortical tension (9) in *Dictyostelium.* Overexpression of RacC induces actin polymerization in spherical protrusions called petalopods and increases phagocytosis rates threefold (29). Recently, Rac1 was also shown to control actin polymerization and other actin-related activities such as macropinocytosis, phagocytosis, chemotaxis, and growth (5, 8, 19). To identify the function of RacB, we conditionally expressed HA-tagged wild-type and mutant versions of RacB in *Dictyostelium.* The data indicate that RacB has a unique function in controlling the actin cytoskeleton, distinguishing this Rac from the three other Rac proteins described so far and supporting our hypothesis that the family of Rac proteins in *Dictyostelium* act in a nonredundant fashion.

Cells overexpressing N17-RacB appeared morphologically normal, while cells overexpressing WT-RacB became flattened. Furthermore, most of the cells expressing V12-RacB became detached from the substrate and formed many surface protrusions, while a small proportion remained attached, became flattened, and showed a similar morphology to WT-RacB overexpressing cells. Cells stopped growing following expression of V12-RacB. V12-RacB expression does not simply inhibit cytokinesis, because the increase in the size of cells and the accumulation of nuclei in cells over time were much smaller than those observed with a myosin II mutation in which cytokinesis is totally blocked. It is more likely that expression of RacB affects cell growth and the cell cycle, as has been suggested for other systems (18, 30).

The surface protrusions produced by V12-RacB cells resemble apoptotic membrane blebs; however, characteristics of apoptosis such as nuclear condensation, chromosome degradation, and phosphatidylserine exposure were not observed in cells overexpressing V12-RacB (E. Lee, unpublished observations). A role for myosin II in apoptotic blebbing has been suggested from studies using the inhibitors of myosin light-chain kinase (13). Consistent with this, BDM, a myosin ATPase inhibitor, stalled the retraction and expansion of apoptotic blebbing (13). BDM treatment eliminated the spherical protrusions in V12-RacB cells, suggesting that the protrusions formed by V12-RacB might be dependent on a myosin ATPase (our unpublished results). However, when V12-RacB was expressed in a myosin II heavy-chain null mutant, protrusions were still formed. Therefore, it is possible that a myosin other than

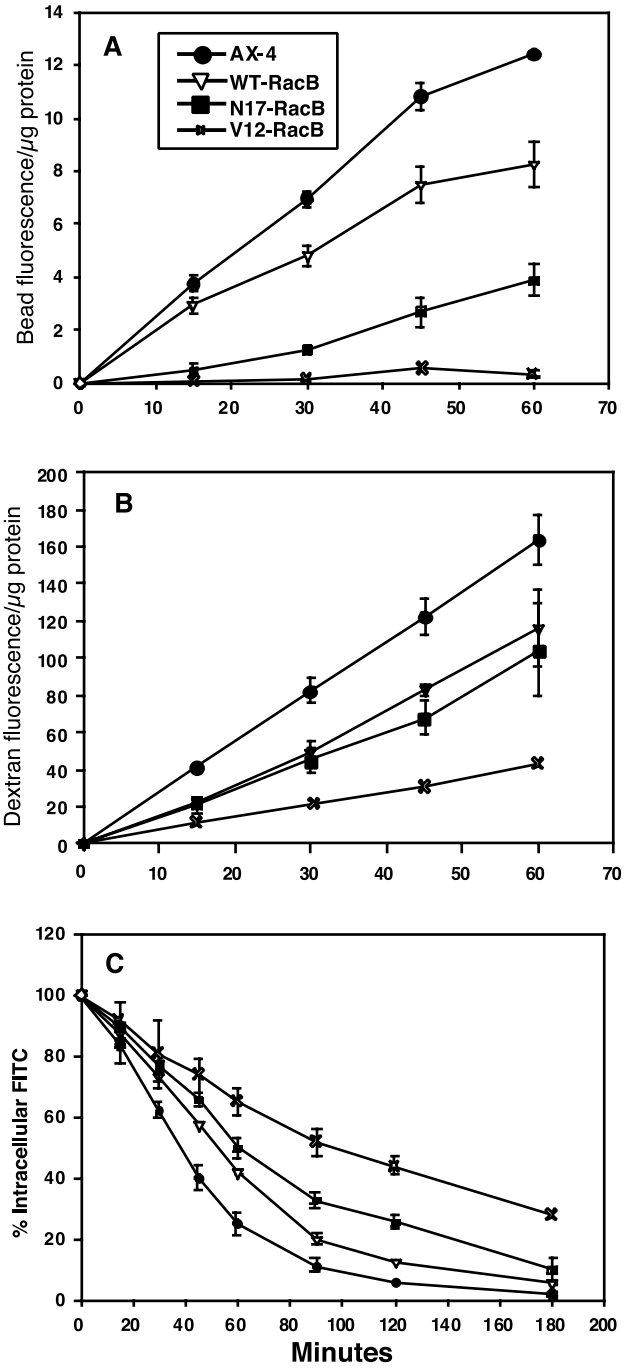

FIG. 9. Quantitation of phagocytosis, macropinocytosis, and recycling rates. (A) Uptake of fluorescent beads by phagocytosis. (B) Uptake of fluorescent dextran by endocytosis. (C) Efflux of the endocytic probe. Efflux was measured by feeding cells with fluorescent dextran for 3 h and then measuring the fluorescence remaining at each time point.

FIG. 8. Visualization of actin dynamics in live cells, using GFP-ABD. (A) Parental Ax4 cells expressing GFP-ABD were observed by confocal microscopy at 20-s intervals. GFP-ABD localizes to the actin cortex and new protrusions as they form at the periphery of the cell (arrow). (B) Cells coexpressing GFP-ABD and V12-RacB were induced for 2 days, and time-lapse images were acquired at 20-s intervals. Cells became detached and actively formed actin-containing spherical protrusions (arrow). (C) Ax4 cells expressing GFP-ABD were electroporated, and the process of bleb formation was visualized by confocal microscopy at 7-s intervals. Note the lack of staining of the bleb. (D) Cells coexpressing GFP-ABD and WT-RacC were induced for 2 days, and time-lapse images were acquired at 20-s intervals. Cells deform the actin cortex both inwardly (arrowhead) and outwardly (arrow). Bar, 5 μm.

myosin II might play a role in the formation of the protrusions induced by V12-RacB. In contrast, blebs formed by wild-type cells under stress were myosin II dependent. Thus, we conclude that the spherical protrusions observed in V12-RacB-expressing cells are a form of protrusion different from the passive blebs found after stress or apoptosis, which are myosin II dependent. Rather, RacB-induced protrusions depend on actin polymerization since cytochalasin A treatment inhibits their formation. Consistent with this, we have observed that the levels of F-actin increase twofold in cells overexpressing V12-RacB.

Both V12-RacB-expressing cells and WT-RacC-expressing cells display surface protrusions; however, there are clear differences in the nature of these structures. V12-RacB expression results in cells detaching from the substratum and induces a threefold increase in the number of protrusions. The protrusions are fairly small and regular and appear to form on top of the existing cortex, so that even with these protrusions, the cells remain overall spherical. Petalopodia are two to four times larger than the protrusions induced by V12-RacB and appear as if the entire cell margin is bulged outward. This difference is shown at the ultrastructural level by the difference in localization of F-actin in the two cell types. The V12-RacB protrusions appear to be actin filled, while the petalopods appear to stain only at the periphery. The fact that WT-RacC induces a significant increase in the phagocytosis rate of cells while V12-RacB causes a nearly complete shutdown in phagocytosis and WT-RacB slightly reduces phagocytosis also supports the idea that these two GTPases have dramatically different consequences for cortical organization and function. However, WT-RacC was expressed constitutively from an actin promoter while V12-RacB was expressed from the inducible discoidin promoter. It is still possible that the amount or mode of expression may affect the phenotypic consequences to the cell. Until more is known about the downstream signaling pathway, the conclusion that these two GTPases affect different actin polymerization pathways remains tentative.

Expression of RacB wild-type and mutant forms also had dramatic effects on trafficking into and along the endolysosomal pathway. Expression of V12-RacB resulted in greater than 75% reductions in the rate of phagocytosis, endocytosis of fluid, and exocytosis of fluid compared to wild-type cells. When phalloidin-stained cells were examined by confocal microscopy, there was no evidence of the crowns normally associated with macropinocytosis on the dorsal surface of V12-RacB cells. It seems likely that the surface protrusions are interfering with normal crown formation and thus with macropinocytosis. This suggests that the inability of the V12-RacB mutant to hydrolyze GTP, and thus to cycle between GTP- and GDP-bound states, leads to a strong mutant phenotype. In contrast, expression of constitutively active RacC (unpublished results) or Rac1B (19) did not significantly affect these processes.

We propose that RacB expression regulates outward protrusions by locally stimulating actin polymerization. In summary, consideration of the data described here for RacB suggests that all of the *Dictyostelium* Rac proteins described thus far, including RacF, RacC, RacE, Rac1, and RacB, play unique roles in regulating F-actin polymerization and generating specific types of actin-containing structures.

ACKNOWLEDGMENTS

We thank Ka Ming Pang for construction of the hygromycin selectable plasmid expressing the GFP-actin binding domain, and for thoughtful comments on the manuscript. We also thank Michael Lynes and Marie Cantino for technical support of FACS analysis and electron microscopy, respectively.

This work was supported by grants from the NIH to D. Knecht (GM 40599) and J. Cardelli (DK 39232).

REFERENCES

1. **Aronheim, A., Y. C. Broder, A. Cohen, A. Fritsch, B. Belisle, and A. Abo.** 1998. Chp, a homologue of the GTPase Cdc42Hs, activates the JNK pathway and is implicated in reorganizing the actin cytoskeleton. Curr. Biol. **8:**1125–1128.
2. **Bishop, A. L., and A. Hall.** 2000. Rho GTPases and their effector proteins. Biochem. J. **348:**241–255.
3. **Blusch, J., P. Morandini, and W. Nellen.** 1992. Transcriptional regulation by folate: inducible gene expression in *Dictyostelium* transformants during growth and early development. Nucleic Acids Res. **20:**6235–6238.
4. **Bush, J., K. Franek, and J. Cardelli.** 1993. Cloning and characterization of seven novel *Dictyostelium discoideum* rac-related genes belonging to the rho family of GTPases. Gene **136:**61–68.
5. **Chung, C. Y., S. Lee, C. Briscoe, C. Ellsworth, and R. A. Firtel.** 2000. Role of Rac in controlling the actin cytoskeleton and chemotaxis in motile cells. Proc. Natl. Acad. Sci. USA **97:**5225–5230.
6. **De Lozanne, A., and J. A. Spudich.** 1987. Disruption of the *Dictyostelium* myosin heavy chain gene by homologous recombination. Science **236:**1086–1091.
7. **Dharmawardhane, S., V. Warren, A. L. Hall, and J. Condeelis.** 1989. Changes in the association of actin-binding proteins with the actin cytoskeleton during chemotactic stimulation of *Dictyostelium discoideum.* Cell Motil. Cytoskeleton **13:**57–63.
8. **Dumontier, M., P. Hocht, U. Mintert, and J. Faix.** 2000. Rac1 GTPases control filopodia formation, cell motility, endocytosis, cytokinesis and development in *Dictyostelium.* J. Cell Sci. **113:**2253–2265.

8a. **Fleurat-Lessard, P., and R. Satter.** 1985. Relationship between structure and motility of Albi22ia motor organs: changes in ultrastructure of cortical cells during dark-induced closure. Protoplasma **128:**72–79.

9. **Gerald, N., J. Dai, H. P. Ting-Beall, and A. De Lozanne.** 1998. A role for *Dictyostelium racE* in cortical tension and cleavage furrow progression. J. Cell Biol. **141:**483–492.
10. **Hall, A.** 1998. Rho GTPases and the actin cytoskeleton. Science **279:**509–514.
11. **Knecht, D. A., and W. F. Loomis.** 1987. Antisense RNA inactivation of myosin heavy chain gene expression in *Dictyostelium discoideum.* Science **236:**1081–1086.
12. **Larochelle, D. A., K. K. Vithalani, and A. De Lozanne.** 1996. A novel member of the rho family of small GTP-binding proteins is specifically required for cytokinesis. J. Cell Biol. **133:**1321–1329.
13. **Mills, J. C., N. L. Stone, J. Erhardt, and R. N. Pittman.** 1998. Apoptotic membrane blebbing is regulated by myosin light chain phosphorylation. J. Cell Biol. **140:**627–636.
14. **Murphy, G. A., P. A. Solski, S. A. Jillian, P. Perez de la Ossa, P. D'Eustachio, C. J. Der, and M. G. Rush.** 1999. Cellular functions of TC10, a Rho family GTPase: regulation of morphology, signal transduction and cell growth. Oncogene **18:**3831–3845.
15. **Neudauer, C. L., G. Joberty, N. Tatsis, and I. G. Macara.** 1998. Distinct cellular effects and interactions of the Rho-family GTPase TC10. Curr. Biol. **8:**1151–1160.
16. **Nobes, C. D., and A. Hall.** 1995. Rho, rac, and cdc42 GTPases regulate the assembly of multimolecular focal complexes associated with actin stress fibers, lamellipodia, and filopodia. Cell **81:**53–62.
17. **Nobes, C. D., I. Lauritzen, M. G. Mattei, S. Paris, A. Hall, and P. Chardin.** 1998. A new member of the Rho family, Rnd1; promotes disassembly of actin filament structures and loss of cell adhesion. J. Cell Biol. **141:**187–197.
18. **Olson, M. F., A. Ashworth, and A. Hall.** 1995. An essential role for Rho, Rac, and Cdc42 GTPases in cell cycle progression through G1. Science **269:**1270–1272.
19. **Palmieri, S. J., T. Nebl, R. K. Pope, D. J. Seastone, E. Lee, E. H. Hinchcliffe, G. Sluder, D. Knecht, J. Cardelli, and E. J. Luna.** 2000. Mutant Rac1B expression in dictyostelium: effects on morphology, growth, endocytosis, development, and the actin cytoskeleton. Cell. Motil. Cytoskeleton **46:**285–304.
20. **Pang, K., E. Lee, and D. Knecht.** 1998. Use of a fusion protein between GFP and an actin-binding domain to visualize transient filamentous-actin structures. Curr. Biol. **8:**405–408.
21. **Pang, K., M. A. Lynes, and D. A. Knecht.** 1999. Variables controlling the expression level of exogenous genes in *Dictyostelium.* Plasmid **41:**187–197.
22. **Paterson, H., A. J. Self, M. D. Garrett, I. Just, K. Aktories, and A. Hall.** 1990.

Microinjection of recombinant p21rho induces rapid changes in cell morphology. J. Cell Biol. **111:**1001–1007.
23. **Rathi, A., S. C. Kayman, and M. Clarke.** 1991. Induction of gene expression in *Dictyostelium* by prestarvation factor, a factor secreted by growing cells. Dev. Genet. **12:**82–87.
24. **Ridley, A. J., and A. Hall.** 1992. The small GTP-binding protein rho regulates the assembly of focal adhesions and actin stress fibers in response to growth factors. Cell **70:**389–399.
25. **Ridley, A. J., H. F. Paterson, C. L. Johnston, D. Diekmann, and A. Hall.** 1992. The small GTP-binding protein rac regulates growth factor-induced membrane ruffling. Cell **70:**401–410.
26. **Rivero, F., R. Albrecht, H. Dislich, E. Bracco, L. Graciotti, S. Bozzaro, and A. A. Noegel.** 1999. RacF1, a novel member of the Rho protein family in *Dictyostelium discoideum,* associates transiently with cell contact areas, macropinosomes and phagosomes. Mol. Biol. Cell **10:**1205–1219.
27. **Roberts, A. W., C. Kim, L. Zhen, J. B. Lowe, R. Kapur, B. Petryniak, A. Spaetti, J. D. Pollock, J. B. Borneo, G. B. Bradford, S. J. Atkinson, M. C. Dinauer, and D. A. Williams.** 1999. Deficiency of the hematopoietic cell-specific Rho family GTPase Rac2 is characterized by abnormalities in neutrophil function and host defense. Immunity **10:**183–196.
28. **Ruppel, K. M., T. Q. P. Uyeda, and J. A. Spudich.** 1994. Role of highly conserved lysine 130 of myosin motor domain. J. Biol. Chem. **269:**18773–18780.
29. **Seastone, D. J., E. Lee, J. Bush, D. Knecht, and J. Cardelli.** 1998. Overexpression of a novel rho family GTPase, RacC, induces unusual actin-based structures and positively affects phagocytosis in *Dictyostelium discoideum.* Mol. Biol. Cell **9:**2891–2904.
30. **Tanaka, T., I. Tatsuno, Y. Noguchi, D. Uchida, T. Oeda, S. Narumiya, T. Yasuda, H. Higashi, M. Kitagawa, K. Nakayama, Y. Saito, and A. Hirai.** 1998. Activation of cyclin-dependent kinase 2 (Cdk2) in growth-stimulated rat astrocytes. Geranylgeranylated Rho small GTPase(s) are essential for the induction of cyclin E gene expression. J. Biol. Chem. **273:**26772–26778.